



OPEN

Effect of surface topography and wettability on shear bond strength of Y-TZP ceramic

Suriyakul Wongsue¹, Ornnicha Thanatvarakorn², Taweesak Prasansuttiporn³✉, Piyarat Nimmanpipug⁴, Thanapat Sastraruji⁵, Keiichi Hosaka⁶, Richard M. Foxton⁷ & Masatoshi Nakajima⁸

Zirconia ceramics have been widely used as dental restorations due to their esthetic appearance and high flexural strength. The bonding of zirconia with resin cement should rely on both mechanical and chemical bonds. This study was performed to investigate the effect of zirconia surface topography and its wettability after surface pretreatments on the microshear bond strength (μ SBS) of a resin cement. Zirconia slabs were prepared and randomly divided into 5 groups based on the surface treatment as follows: no treatment (control), air abrasion (AB), etching with hydrofluoric acid (F), the mixture of hydrofluoric acid and nitric acid (FN), or the mixture of hydrochloric acid and nitric acid (CN) for 10 min. The specimens were subjected to investigation of surface roughness characteristics [average roughness (Ra), peak-to-valley average distance (Rpv), skewness (Rsk), and kurtosis (Rku)] using atomic force microscopy (AFM) and measurements of surface contact angle (θ_c) and μ SBS of a resin cement. In addition, the area % of the nanoscale surface irregularity (nSI%) was calculated from the AFM images. The effects of nSI%, Ra and θ_c on the μ SBS were analyzed by multiple linear regression analysis ($p < 0.05$). Multiple regression analysis revealed that the nSI% was the most predominant factor for the μ SBS ($p < 0.001$). A surface with larger nSI%, higher Ra and relatively lower θ_c was essential for establishing a reliable resin-zirconia bond.

Yttria-stabilized tetragonal zirconia polycrystal (Y-TZP) ceramics have been widely used in restorative dentistry due to their esthetic appearance and high flexural strength¹. However, the bonding of zirconia with resin cement is still considered problematic. Unlike glass ceramics, these ceramics cannot be etched with conventional 5–9% hydrofluoric acid (HF) to create the surface roughness necessary for mechanical interlocking. Thus, the standard protocol is airborne-particle abrasion for mechanically roughening the surface^{2,3}, accompanied by the application of 10-methacryloyloxydecyl dihydrogen phosphate (10-MDP) monomer to facilitate chemical bonding⁴. This protocol has been reported to be successful in achieving optimal zirconia-resin bond strength and bond durability^{5–7}.

However, air abrasion was reported to produce sharp-edged irregularities, which might cause initiation of crack propagation in the material⁸. Moreover, a too deep and narrow rough surface of adherend materials would reduce the penetration of adhesives or resin cements^{9,10}, leading to prevention of the optimal formation of mechanical interlocking and/or chemical bonding. Meanwhile, it was speculated that a shallow and wide-open rough surface would be more favorable in allowing complete filling of resin cement¹¹.

Concurrently, HF at a high concentration was introduced to etch the zirconia and provide roughness on the zirconia surface, manifested as micro- and nano-porosity^{11,12}. Although the formation of nano-porosity did not

¹Dental Section, Buddhasothorn Hospital, Na Muang, Muang 24000, Chachoengsao, Thailand. ²Faculty of Dentistry, Bangkokthonburi University, 16/10 Leab Klong Taweewatana Rd., Taweewatana 10170, Bangkok, Thailand. ³Department of Restorative Dentistry and Periodontology, Faculty of Dentistry, Chiang Mai University, Suthep, Muang Chiang Mai 50200, Chiang Mai, Thailand. ⁴Department of Chemistry, Faculty of Science, Chiang Mai University, Suthep, Muang Chiang Mai 50200, Chiang Mai, Thailand. ⁵Dental Research Center, Faculty of Dentistry, Chiang Mai University, Suthep, Muang Chiang Mai 50200, Chiang Mai, Thailand. ⁶Department of Regenerative Dental Medicine, Graduate School of Biomedical Sciences, Tokushima University, 3-18-15, Kuramoto-cho, Tokushima 770-8504, Japan. ⁷King's College London Dental Institute, King's College London, Floor 25, London Bridge, London SE1-9RT, UK. ⁸Department of Cariology and Operative Dentistry, Graduate School of Medical and Dental Sciences, Tokyo Medical and Dental University, 1-5-45, Yushima, Bunkyo-ku, Tokyo 113-8549, Japan. ✉email: dent.taweesak@gmail.com

drastically increase the average surface roughness (Ra) value, compared to air abrasion, its presence was found to increase surface wettability and improve the resin-zirconia bond strength¹¹.

Regarding roughness measurement, zirconia bonding studies generally report treated zirconia surface topography by the Ra value, which evaluates the surface irregularities in the vertical direction. It should be noted that Ra only measures the height average deviation from the mean line, where the slopes, sizes, geometries of peaks and valleys, or nanoscale irregularity on the microrough surface cannot be exactly detailed¹³. Therefore, other surface roughness parameters, such as the average distance from the tips of peaks to valleys (Rpv), the height distribution and tip geometry of peaks and valleys evaluated by skewness (Rsk) and kurtosis (Rku), and the presence of nanoscale surface irregularity (nSI), should be investigated because they might be able to affect resin penetration and, consequently, the resin-zirconia bond strength.

Thus, the objective of this study was to investigate the effect of surface topography, determined by Ra, Rpv, Rsk, and Rku, the surface wettability, and the nSI of pretreated zirconia ceramics on the microshear bond strengths (μ SBS) of a resin cement to zirconia. The null hypothesis tested was that the surface topography and wettability do not affect resin-zirconia bond strengths.

Methods

Zirconia specimen preparation and surface treatment

Sixty zirconia slabs were prepared from partially-sintered zirconia milling blanks (BruxZir[®] Shaded; Glidewell Laboratories, CA, USA) by using a low-speed diamond saw (IsoMet[™] low speed cutter; Buehler, IL, USA), and the top and bottom surfaces of slabs were polished under water running with abrasive SiC papers (600, 800, 1000, 1200, and 2000 grits, respectively) using a grinding machine (MoPao[™] 160E, Laizhou Weiyi, Shandong, China). Then, all the specimens were fully sintered into the final dimensions of 10 × 10 × 2 mm following the manufacturer's instructions and randomly assigned into 5 groups (n = 12) as follows: Control: no surface treatment, Group AB: air abrasion with 50 μ m alumina particles under 2 bars at 10 mm from the specimen top surface for 10 s followed by 10 min ultrasonic cleaning in deionized water, Group F: etching with 48% HF, Group FN: etching with 48% HF mixed with 68% nitric acid (HNO₃) at a 1:1 ratio by volume, and Group CN: etching with 37% hydrochloric acid (HCl) mixed with 68% HNO₃ at a 4:1 ratio by volume. In the acid etching groups, 50 μ L of designated acid was dropped and thus wetted the zirconia surface for 10 min, followed by rinsing with deionized water for 1 min. The chemical agents used are listed in Table 1. To eliminate the variation in surface chemistry in each treatment, carbon was intentionally allowed to absorb on the specimen surfaces by storing the specimens in an empty closed container at room temperature for 21 days before the following experiments.

Surface topography assessment using atomic force microscopy (AFM)

Surface roughness characteristics measurement

All the specimens were investigated for surface roughness characteristics using AFM (PARK XE7, Park Systems, Gyeonggi, South Korea) in noncontact mode. The parameters Ra, Rpv, Rsk, and Rku were calculated using analysis software (XEI 4.3, Park Systems, Gyeonggi, South Korea). The Ra, Rpv, Rsk, and Rku data were analyzed statistically with one-way ANOVA and Tukey's test ($p < 0.05$).

Rsk is a measure of the asymmetry of the profile about the mean line calculated over the evaluation length. Profiles with predominant deep valleys have negative skewness, whereas those with several high peaks show positive values. Rku is a measure of the peakedness of the profile about the mean line calculated over the evaluation length. It describes the sharpness of the probability density of the profile, of which $Rku > 3$ indicates sharp peaks and valleys, and $Rku < 3$ refers to relatively flat peaks and valleys. If $Rku = 3$, then the curve is Gaussian (Fig. 1)¹⁴.

Agents	Manufacturer	Composition	Application
HF (Emsure [®] Hydrofluoric acid)	Merck, Darmstadt, Hesse, Germany [B1004344747]	48% w/w HF	–
HNO ₃ (Gammaco [™] Nitric acid)	Gammaco, Bang Kruai, Nonthaburi, Thailand [3095045]	68% w/w HNO ₃	–
HCl (Emsure [®] Hydrochloric acid)	Merck, Darmstadt, Hesse, Germany [K45311117505]	37% w/w HCl	–
Clearfil [™] Ceramic Primer Plus	Kuraray Noritake Inc., Okayama, Japan [AU0049]	3-trimethoxysilylpropyl methacrylate, 10-MDP, Ethanol	Apply primer on zirconia surface and allow it to react for 10 s, then dry with mild air flow
Panavia [™] V5; Dual cure mode, Clear color	Kuraray Noritake Inc., Okayama, Japan [7S0027]	Bis-GMA, TEGDMA, Hydrophobic aromatic dimethacrylate, hydrophilic aliphatic dimethacrylate, initiators, accelerators, silanated barium glass filler, silanated fluoroaluminosilicate glass filler, colloidal silica, silanated aluminium oxide filler, dl-camphorquinone, pigments	1. Attach a mixing tip to the syringe 2. Load mixed paste into polyethylene mold placed over zirconia surface 3. Remove excess cement, and light-cure for 20 s

Table 1. Materials used in this study. HF Hydrofluoric acid, HNO₃ Nitric acid, HCl Hydrochloric acid, 10-MDP 10-Methacryloyloxydecyl dihydrogen phosphate, Bis-GMA 2,2-Bis[4-(2-hydroxy-3-methacryloyloxypropoxy)-phenyl] propane, TEGDMA Triethyleneglycol dimethacrylate.

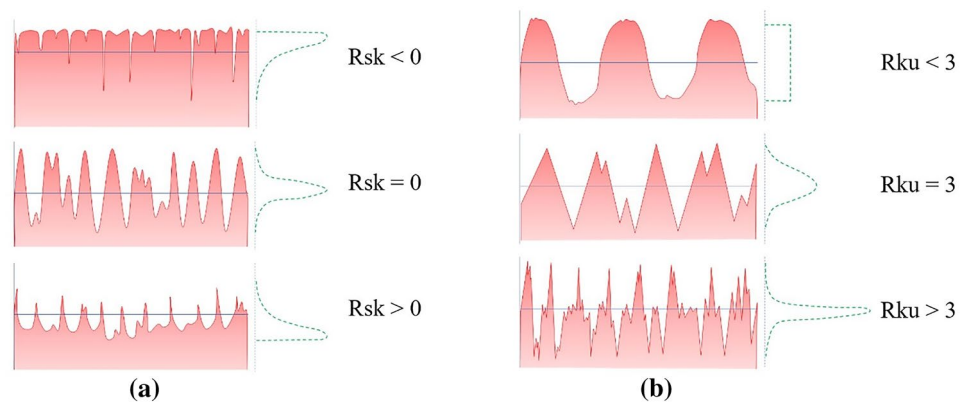


Figure 1. Schematic illustrations demonstrate the meaning of parameters Rsk (a) and Rku (b).

nSI assessment

To observe nanoscale surface topography, a $5 \times 5 \mu\text{m}$ -AFM image with 256×256 pixels was taken with a scan rate of 0.5 Hz to assess nSI on the treated zirconia surface. The nSI area was quantitatively defined as a percentage of the whole surface (nSI%) by manual counting using a simple hundred-square grid from a 2D image. If a clearly smooth grain surface presented more than 50% of the square grid, it was counted as a smooth grain surface grid (Fig. 2a). Meanwhile, if the rough or irregular grain surface presented more than 50% of the square grid, it was counted as an nSI grid (Fig. 2b).

Twelve images from each group were measured by 2 observers, 2 times with a 1-week interval. A validation of the method used in this study was performed by both intraobserver and interobserver reliability analysis using the intraclass correlation coefficient (ICC) test, whose correlation ratios were 0.988 and 0.972, respectively ($p < 0.05$). The nSI% was analyzed statistically with one-way ANOVA and Tukey's test ($p < 0.05$).

Surface contact angle (θ_c) assessment

All the treated specimens were used for contact angle measurement by the sessile drop technique. One microliter of deionized water was dropped on the specimen surface and left for 1 min prior to the measurement using a goniometer (CMU-PHYS™ Goniometer, CMU-PHYSnanolabs, Chiang Mai, Thailand). The θ_c data were analyzed statistically with one-way ANOVA and Tukey's test ($p < 0.05$).

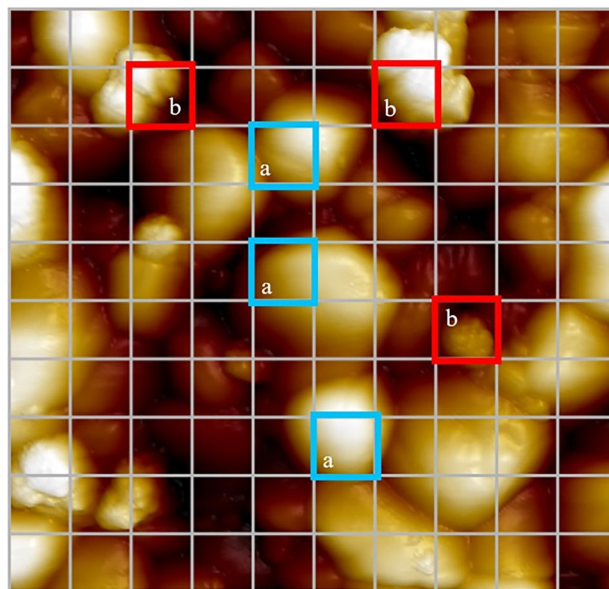


Figure 2. The representative $5 \times 5 \mu\text{m}$ zirconia surface in a 2D image, showing the counting from a hundred-square grid. Blue squares (a) show smooth grain surface grids, and red squares (b) show nanoscale surface irregularity (nSI) grids.

μSBS test

After the investigations, all the specimen surfaces were applied with a 10-MDP containing primer (Clearfil™ Ceramic Primer Plus, Kuraray Noritake Inc., Okayama, Japan). After placing polyethylene tubes (Tygon®, Norton Performance Plastic, OH, USA) with an internal diameter of 0.8 mm and a height of 0.5 mm on the zirconia surface, resin cement (Panavia™ V5, Kuraray Noritake Inc., Okayama, Japan) was subsequently injected into the tube and light cured for 20 s from the top surface using a light-curing unit (Bluephase® N, Ivoclar Vivadent, Schaan, Liechtenstein). All specimens were stored in 37 °C distilled water for 24 h. After carefully removing the tubes, the specimens were subjected to μSBS testing using a universal testing machine (Instron® 5566, Illinois Tool Works, MA, USA) using the wire-loop technique at a crosshead speed of 0.5 mm/min. The materials used are listed in Table 1. The μSBS data were analyzed statistically with one-way ANOVA and Tukey's test ($p < 0.05$).

Failure mode analysis

After the μSBS test, failure mode analysis was carried out using a stereoscopic microscope (Olympus™ SZX7, Olympus, Tokyo, Japan) at 56× magnification. Failure modes were categorized into 3 types as follows¹⁵: *adhesive failure* (80–100% of the failure occurred at the interface between resin cement and zirconia), *cohesive failure* in resin cement or zirconia (80–100% of the failure occurred within resin cement or zirconia), and *mixed failure* (mixed with adhesive and cohesive failure patterns in the same specimen). The failure mode data were analyzed statistically with the chi-square test ($p < 0.05$).

Multiple linear regression analysis

To investigate the effect of nSI%, Ra and θ_c on μSBS, multiple regression analysis was performed by using IBM SPSS Statistics version 27.0 (IBM, Chicago, IL, USA) ($p < 0.05$). Model fit was assessed using the coefficient of determination (R squared).

Results

Surface topography assessment using AFM

The means of Ra, Rpv, Rsk, Rku and their standard deviations are presented in Table 2. All the surface treatments exhibited significant increases in Ra and Rpv values compared with the control group ($p < 0.05$). The AB and F groups exhibited the highest Ra and Rpv values among the treatments. The Rsk values were negative in the control and CN groups, whereas they were near zero in the AB group and positive in the F and FN groups. The Rku value of the control group was more than 3. All the surface treatments caused an insignificant change in Rku compared with the control group ($p > 0.05$). The only significant difference in Rku was found between the CN group (highest Rku, more than 3) and the F group (lowest Rku, less than 3) ($p < 0.05$).

Representative AFM images exhibiting the surface topography of nontreated and surface-treated zirconia are shown in Fig. 3. Smooth surface grains and grain boundaries were clearly observed in the control group. On the other hand, the F and FN groups clearly exhibited nSI on grains with unclear grain boundaries. In the AB group, nSI with unclear grain boundaries was observed in the lesser amount. For the CN group, small protrusions were observed on the smooth surface grains with traceable boundaries.

The means and standard deviations of nSI% are shown in Table 2. All the treatments significantly increased nSI% compared with the control group ($p < 0.05$), and the F and FN groups showed significantly higher nSI% than the AB and CN groups ($p < 0.05$).

θ_c assessment

The mean θ_c and standard deviations are shown in Table 2. All the surface treatments significantly decreased θ_c compared with the control group ($p < 0.05$), in which the FN group exhibited significantly lower θ_c among the treatment groups ($p < 0.05$).

μSBS test

The means and standard deviations of μSBS in each group are shown in Table 2. All the treatments significantly increased μSBS compared with the control group ($p < 0.05$), and the F group exhibited significantly higher μSBS among the treatment groups ($p < 0.05$).

Surface treatments	Surface roughness parameters				nSI%	θ_c (°)	μSBS (MPa)
	Ra (nm)	Rpv (nm)	Rsk	Rku			
Control	47.17 ± 5.44 ^a	448.62 ± 78.38 ^a	-0.23 ± 0.28 ^a	3.22 ± 0.62 ^{ab}	16.33 ± 10.36 ^a	83.33 ± 3.22 ^d	8.59 ± 1.22 ^a
AB	109.39 ± 7.82 ^c	974.56 ± 224.42 ^c	0.00 ± 0.21 ^{abc}	3.14 ± 0.51 ^{ab}	81.00 ± 7.07 ^c	73.18 ± 6.06 ^c	19.37 ± 2.58 ^c
F	104.16 ± 7.55 ^c	893.74 ± 148.61 ^c	0.09 ± 0.21 ^{bc}	2.87 ± 0.32 ^a	92.17 ± 6.59 ^d	63.22 ± 5.71 ^b	22.21 ± 2.35 ^d
FN	73.16 ± 7.59 ^b	706.78 ± 140.88 ^b	0.17 ± 0.27 ^c	3.02 ± 0.48 ^{ab}	91.25 ± 8.29 ^d	53.19 ± 7.59 ^a	19.26 ± 2.00 ^c
CN	69.13 ± 7.55 ^b	648.91 ± 142.96 ^b	-0.21 ± 0.39 ^{ab}	3.53 ± 0.69 ^b	64.33 ± 8.92 ^b	72.76 ± 5.77 ^c	13.78 ± 1.80 ^b

Table 2. Means and standard deviations of surface roughness parameters (Ra, Rpv, Rsk, Rku), area percentage of nanoscale grain-surface irregularity (nSI%), surface contact angle (θ_c) and microshear bond strengths (μSBS) of each group ($n = 12$). Different superscript letters indicate statistically significant differences between surface treatments ($p < 0.05$).

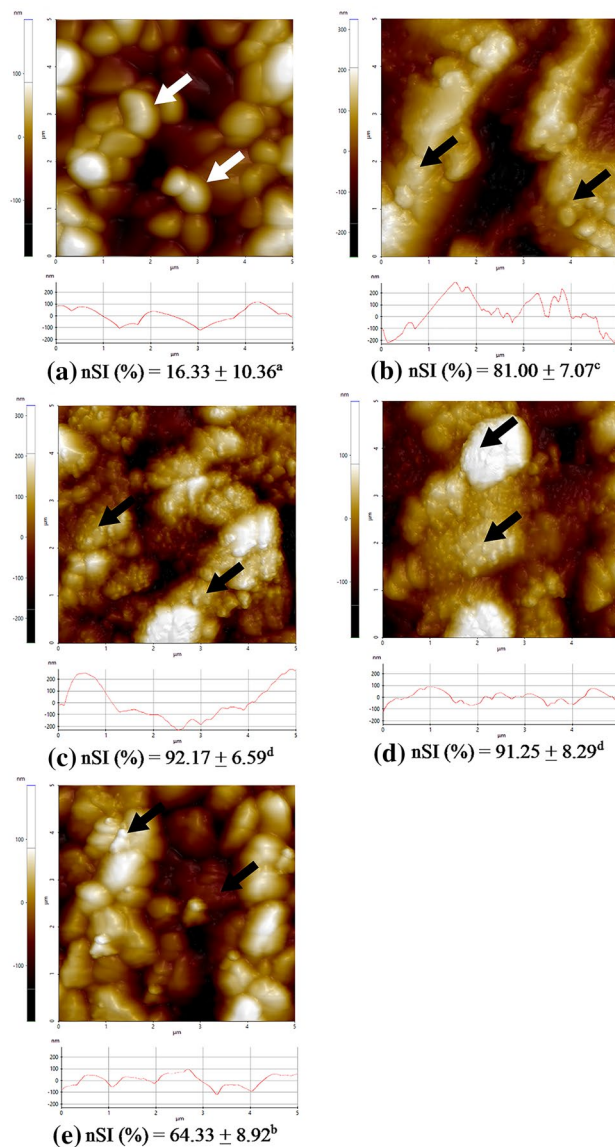


Figure 3. Representative AFM images (upper) and line-scan profiles (lower) of the control (a), AB (b), F (c), FN (d), and CN (e) groups. Grain boundaries (white arrow) were clearly observed in the control group, whereas surface irregularities on grains (black arrows) were observed in all treated groups.

Failure mode analysis

The failure mode distribution is displayed in Fig. 4. The results of the chi-square test revealed that there were significant differences in the failure mode distribution among the groups ($p < 0.05$). The majority of the failure mode of the control was adhesive failure, whereas it was mixed failure in the AB, F, FN, and CN groups.

Multiple linear regression analysis

The regression model with nSI%, Ra and θ_c was significantly fitted to μSBS [$\mu\text{SBS} = 9.487 + 0.089(\text{nSI}\%) + 0.080(\text{Ra}) - 0.079(\theta_c)$] ($p = 0.003$; $R^2 = 0.831$), in which nSI%, Ra, and θ_c were statistically significant predictors ($p < 0.001$, $p < 0.001$ and $p = 0.035$, respectively). The nSI% was the most predominant factor for resin-zirconia bond strength (standardized coefficient beta = 0.499) (Table 3).

Discussion

The results of this study revealed that the air-abrasive and acid-etching treatments used in this study caused variations in the surface topography (Ra, Rpv, Rsk, Rku and nSI%) of the zirconia surface and affected the θ_c and bonding performance of the resin cement. Additionally, nSI%, Ra and θ_c significantly affected μSBS between resin and zirconia. Thus, the null hypothesis was rejected.

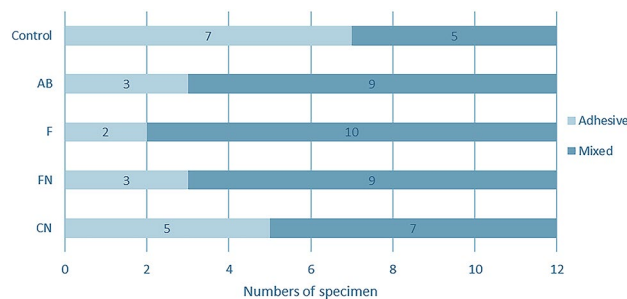


Figure 4. Frequency of failure modes after μ SBS testing in each group ($n = 12$). The numbers in each bar are the numbers of specimens in each failure mode. There were significant differences in the failure mode distribution among the groups ($p < 0.05$). The majority of the failure mode of the control was adhesive failure, whereas it was mixed failure in the AB, F, FN, and CN groups.

Model	Sum of squares	df	Mean square	F	Sig.
ANOVA					
Regression	1371.053	3	457.018	91.479	<0.001
Residual	279.769	56	4.996		
Total	1650.823	59			
Model	Unstandardized coefficients		Standardized coefficients	Sig.	Collinearity statistics
	B	Std. Error	Beta		VIF
Constant	9.487	3.090		0.003	
nSI%	0.089	0.020	0.499	<0.001	3.960
Ra	0.080	0.018	0.367	<0.001	2.332
θ_c	-0.079	0.036	-0.174	0.035	2.146

Table 3. Multiple linear regression analysis. $R^2 = 0.831$.

AFM was employed in this study since it is an essential tool for characterizing surface topography, particularly on the nanoscale, providing a direct view of surface features at high resolution without surface coating being required¹⁶.

With the aim of creating zirconia surfaces with various micro- and nanoscale irregularities, the treatments of airborne particle abrasion or acid etching with HF and its mixture with HNO_3 , including a mixture of HCl with HNO_3 , were used. Air-pressurized abrasion can roughen the surface with large surface defects and mechanically damage the zirconia grains in the top 1- to 1.5- μm zone¹⁷. HF etching using a high concentration can corrode both intergranular and intragranular parts of the zirconia surface, being slightly faster at the grain boundaries¹⁸, leading to a size reduction and dislodgement of zirconia grains¹². These two methods increased Ra and Rpv to the highest values, whereas the mixture of HF with HNO_3 (FN group) and the mixture of HCl with HNO_3 (CN group) caused the lesser increase in Ra and Rpv. The results of this study were consistent with previous studies, which reported that the mixture of HF with HNO_3 was capable of roughening a zirconia surface^{2,19,20} but to a lesser extent than HF etching alone²¹. It was speculated that adding HNO_3 reduced the penetration of the mixture into grain boundaries, no longer dislodging the deeper-part grains. Last, the mixture of HCl with HNO_3 barely etched the zirconia substrate, although its strong oxidative effect²² and its ability to readily dissolve common metallic oxides and hydroxides²³ have been addressed.

In adhesive dentistry, adequate surface wetting of the adhesive on the substrate is the primary requirement to achieve good adhesion²⁴. Good surface wetting, determined by a low contact angle, leads to intimate contact between adhesive and adherend and enhances mechanical interlocking^{25,26}. Thus, surface wettability could be one of the parameters used to predict bonding efficacy. It has been documented that the contact angle is the parameter manifested from the substrate's surface roughness and surface chemistry²⁷. To eliminate the effect of chemical heterogeneity on the treated surfaces, each specimen was stored in a closed container for 21 days before contact angle measurement. This aging condition possibly exerted airborne hydrocarbon adsorption, which subsequently increased the contact angle^{27,28}. Although this method overestimated the values of measured θ_c , it aided the surface chemistry of all treated groups to be homogenized, and hence, the wettability derived from the effect of surface topography could be predominant²⁹.

The Wenzel theory states that an increase in surface roughness could decrease the contact angle for a hydrophilic surface^{30,31}. However, several studies demonstrated that the contact angle decreases following increasing roughness to a certain extent, where no greater improvement in wetting is expected for highly rough surfaces^{32,33}. It should be noted that the wettability was determined not only by the average surface roughness but also by the surface geometry in three dimensions, such as the distance between peaks compared to their height, of which

the proper distance and height could facilitate the liquid to better wet the surface by forming a capillary action³². Excessively high peaks and symmetrically distributed high peaks and deep valleys (near-zero Rsk) conversely decrease wettability (increase θ_c) due to trapped air in surface cavities^{33,34}, whereas flat-shaped peaks and valleys (Rku < 3) are more favourable for enhancing surface wettability³⁵. From the results of this study, the FN group exhibited the lowest θ_c , which could be attributed to an optimal height and a predominance of peaks (positive Rsk) having a symmetric Gaussian shape (Rku = 3). On the other hand, both the AB and F groups created higher rough surfaces, which might be too high, with a more symmetric topography (near-zero Rsk). Thus, the wettability of the AB and F groups was hampered compared to that of the FN group. When compared to each other, the shape of peaks and valleys was relatively sharp in the AB group (Rku > 3) and flat in the F group (Rku < 3), leading to the better wettability of the F group than that of the AB group. Last, the θ_c values of the control and CN groups were the highest among the studied groups due to their low surface roughness and predominance of sharp valleys (negative Rsk and Rku > 3). Presumably, the moderately high roughness, with flat peaks (greater skewness and small kurtosis), might be preferable to enhance liquid wettability on the zirconia surface.

Interestingly, nSI was obviously observed on the grain surfaces of treated zirconia, especially in the F and FN groups. Since this nSI could not be quantified by the roughness parameters described above, the nSI% was evaluated manually by counting under the hundred-square grid method. It was speculated that a zirconia surface with a higher nSI% could increase the surface area for adhesion; thus, a higher bond strength could be expected. Accordingly, the F and FN groups, including the AB group, which had a high nSI%, demonstrated a higher μ SBS than the groups with a lower nSI%.

Regarding the μ SBS results, the highest μ SBS was found in the F group, although its wettability was not the highest. The AB group had comparable μ SBS to the FN group, despite its lower wettability and lower nSI% than that of FN. These results indicated that not only the wettability, defined by θ_c , and the nSI%, but also the surface roughness (Ra), which was highest in the F and AB groups, could cooperatively contribute to improving the bond strength of resin cement to zirconia. This speculation was confirmed by the multiple regression analysis, revealing that nSI%, Ra and θ_c significantly affected the μ SBS ($p < 0.001$, $p < 0.001$ and $p = 0.035$, respectively), in which nSI% was the most predominant factor contributing to the bonding to zirconia (standardized coefficient beta = 0.499), and Ra was a more significant predictor than θ_c (standardized coefficient beta = 0.367 and -0.174, respectively) (Table 3). Therefore, the surface roughness would be an essential parameter for bonding with mechanical interlocking by resin tags to the zirconia surface, and the surface wettability would assist their optimal formation. In this analysis, the variance inflation factor (VIF) value of each predictor was less than 5 (Table 3), which indicates that the multicollinearity between the variables of nSI%, Ra and θ_c was small. Therefore, the nSI% would not be strongly associated with the wettability on the surface.

It is noteworthy that all the surface treatments could increase bond strengths compared with the control group. These findings are in agreement with other studies^{21,36,37}, indicating that roughness is indispensable for the mechanical bond of resin-zirconia. Unlike the results from this study, a higher bond strength of air abrasion over HF treatment has been reported^{21,38}. Additionally, some studies have demonstrated that the use of HF/HNO₃ could increase bond strength to a larger degree than air abrasion^{19,37}. These inconsistent results could be attributed to the differences in acid concentration, etching time, or resin cement types^{19,39,40}. In particular, the 3-week waiting period prior to cementation in this study might affect the chemical bonds of each treatment to different degrees.

Within the methodology in the current study, there are some clinical limitations to be considered. First, it would be impractical to treat the intaglio surface of a crown and wait 3 weeks before proceeding with cementation. Second, the hazards of HF are well recognized⁴¹. Working with highly concentrated HF requires an isolated workspace with adequate ventilation, which is unfeasible in general clinical practice. Finally, the tetragonal-to-monoclinic (*t-m*) phase transformation, which is a critical consideration for the surface treatment of Y-TZP ceramics, was not evaluated in this study. Previous studies demonstrated that gentle air abrasion protocols, as used in this study, generally trigger *t-m* phase transformation⁴²⁻⁴⁴, whereas HF etching with conditions close to the current study was found to induce phase transformation to the lesser degree than air abrasion⁴⁵. Nevertheless, such a small amount of monoclinic phase presented on the zirconia surfaces prior to the bonding procedure was found to not influence the resin bond strength⁴⁵⁻⁴⁷.

After aging, the increase in monoclinic contents⁴⁸ and the decrease in bond strengths of resin-zirconia^{45,49,50} were widely reported. However, the study revealing the negative correlation between monoclinic contents and bond strengths after aging is scarce. On the other hand, some previous studies showed increased monoclinic contents without a significant drop in resin bonding^{51,52}. It was concluded that the effect of resin hydrolysis is responsible for the decreased bond strength more than the phase transformation^{21,52}. Moreover, it is still controversial whether the development of residual stresses at the interface following phase transformation may negatively affect surface adhesion^{47,50}. Therefore, further study investigating the effect of *t-m* phase transformation on both immediate and long-term bond strengths is needed.

It could be concluded based on this *in vitro* study that appropriate surface topography and surface wettability are essential for establishing reliable resin-zirconia bond strength. Of all the factors evaluated, nSI% was the most predominant factor, whereas Ra and θ_c could concomitantly affect the bond strengths of resin cement to zirconia. The surface roughness properties Rsk and Rku are important parameters for facilitating surface wettability.

Data availability

The datasets generated during and/or analysed during the current study are available from the corresponding author on reasonable request.

Received: 27 May 2023; Accepted: 20 October 2023

Published online: 25 October 2023

References

- Piconi, C. & Maccauro, G. Zirconia as a ceramic biomaterial. *Biomaterials* **20**, 1–25. [https://doi.org/10.1016/s0142-9612\(98\)00010-6](https://doi.org/10.1016/s0142-9612(98)00010-6) (1999).
- Goyata, F. *et al.* Effect of surface treatments with acid solutions on the surface roughness of an Yttrium-Tetragonal Zirconia Polycrystal. *J. Clin. Exp. Dent.* **10**, e367–e370. <https://doi.org/10.4317/jced.54571> (2018).
- Paes, P. N. G., Bastian, F. L. & Jardim, P. M. The influence of Y-TZP surface treatment on topography and ceramic/resin cement interfacial fracture toughness. *Dent. Mater.* **33**, 976–989. <https://doi.org/10.1016/j.dental.2017.06.004> (2017).
- Nagaoka, N. *et al.* Chemical interaction mechanism of 10-MDP with zirconia. *Sci. Rep.* **7**, 45563. <https://doi.org/10.1038/srep45563> (2017).
- Ozcan, M. & Bernasconi, M. Adhesion to zirconia used for dental restorations: A systematic review and meta-analysis. *J. Adhes. Dent.* **17**, 7–26. <https://doi.org/10.3290/j.jad.a33525> (2015).
- Tzanakakis, E. G., Tzoutzas, I. G. & Koidis, P. T. Is there a potential for durable adhesion to zirconia restorations? A systematic review. *J. Prosthet. Dent.* **115**, 9–19. <https://doi.org/10.1016/j.prosdent.2015.09.008> (2016).
- Quigley, N. P., Loo, D. S. S., Choy, C. & Ha, W. N. Clinical efficacy of methods for bonding to zirconia: A systematic review. *J. Prosthet. Dent.* **125**, 231–240. <https://doi.org/10.1016/j.prosdent.2019.12.017> (2021).
- Moon, J. E., Kim, S. H., Lee, J. B., Ha, S. R. & Choi, Y. S. The effect of preparation order on the crystal structure of yttria-stabilized tetragonal zirconia polycrystal and the shear bond strength of dental resin cements. *Dent. Mater.* **27**, 651–663. <https://doi.org/10.1016/j.dental.2011.03.005> (2011).
- Borsellino, C., Di Bella, G. & Ruisi, V. F. Adhesive joining of aluminium AA6082: The effects of resin and surface treatment. *Int. J. Adhes. Adhes.* **29**, 36–44. <https://doi.org/10.1016/j.ijadhadh.2008.01.002> (2009).
- Budhe, S., Ghumatkar, A., Birajdar, N. & Banea, M. Effect of surface roughness using different adherend materials on the adhesive bond strength. *Appl. Adhes. Sci.* **3**, 8. <https://doi.org/10.1186/s40563-015-0050-4> (2015).
- Lee, M. H., Son, J. S., Kim, K. H. & Kwon, T. Y. Improved resin-zirconia bonding by room temperature hydrofluoric acid etching. *Materials (Basel)*. **8**, 850–866. <https://doi.org/10.3390/ma8030850> (2015).
- Sriamporn, T. *et al.* Dental zirconia can be etched by hydrofluoric acid. *Dent. Mater. J.* **33**, 79–85. <https://doi.org/10.4012/dmj.2013-243> (2014).
- Bhushan, B. Surface roughness analysis and measurement techniques. In *Modern Tribology Handbook* (ed. Bhushan, B.) 49–119 (CRC Press, 2000).
- Ba, E. C. T. *et al.* Investigation of the effects of skewness Rsk and kurtosis Rku on tribological behavior in a pin-on-disc test of surfaces machined by conventional milling and turning processes. *Mater. Res.* **24**, e20200435 (2021).
- Thammajaruk, P., Buranadham, S., Thanatvarakorn, O. & Guazzato, M. Influence of nano-structured alumina coating on composite-zirconia bonding and its characterization. *J. Adhes. Dent.* **20**, 233–242. <https://doi.org/10.3290/j.jad.a40512> (2018).
- Wang, H. & Chu, P. K. Surface characterization of biomaterials. In *Characterization of Biomaterials* (eds Bandyopadhyay, A. & Bose, S.) 105–174 (Academic Press, 2013).
- Inokoshi, M. *et al.* Structural and chemical analysis of the zirconia-veneering ceramic interface. *J. Dent. Res.* **95**, 102–109. <https://doi.org/10.1177/0022034515608825> (2016).
- Flamant, Q., García Marro, F., Roa Rovira, J. J. & Anglada, M. Hydrofluoric acid etching of dental zirconia. Part 1: Etching mechanism and surface characterization. *J. Eur. Ceram. Soc.* **36**, 121–134. <https://doi.org/10.1016/j.jeurceramsoc.2015.09.021> (2016).
- Cho, J. H., Kim, S. J., Shim, J. S. & Lee, K. W. Effect of zirconia surface treatment using nitric acid-hydrofluoric acid on the shear bond strengths of resin cements. *J. Adv. Prosthodont.* **9**, 77–84. <https://doi.org/10.4047/jap.2017.9.2.77> (2017).
- Lee, Y., Oh, K. C., Kim, N. H. & Moon, H. S. Evaluation of zirconia surfaces after strong-acid etching and its effects on the shear bond strength of dental resin cement. *Int. J. Dent.* **2019**, 3564275. <https://doi.org/10.1155/2019/3564275> (2019).
- Liu, D., Tsoi, J. K., Matinlinna, J. P. & Wong, H. M. Effects of some chemical surface modifications on resin zirconia adhesion. *J. Mech. Behav. Biomed. Mater.* **46**, 23–30. <https://doi.org/10.1016/j.jmbbm.2015.02.015> (2015).
- Green, T. A. Gold etching for microfabrication. *Gold Bull.* **47**, 205–216. <https://doi.org/10.1007/s13404-014-0143-z> (2014).
- Craig, B. & Anderson, D. *Handbook of Corrosion Data* 2nd edn. (ASM International, 1995).
- Van Meerbeek, B., Yoshihara, K., Van Landuyt, K., Yoshida, Y. & Peumans, M. From Buonocore's pioneering acid-etch technique to self-adhering restoratives. A status perspective of rapidly advancing dental adhesive technology. *J. Adhes. Dent.* **22**, 7–34. <https://doi.org/10.3290/j.jad.a43994> (2020).
- Zain, N., Ahmad, S. & Suzana, E. Enhancement of adhesive bonding strength: Surface roughness and wettability characterisations. *J. Mech. Eng.* **11**, 55–73 (2014).
- Piascik, J. R., Swift, E. J., Braswell, K. & Stoner, B. R. Surface fluorination of zirconia: Adhesive bond strength comparison to commercial primers. *Dent. Mater.* **28**, 604–608. <https://doi.org/10.1016/j.dental.2012.01.008> (2012).
- Noro, A., Kaneko, M., Murata, I. & Yoshinari, M. Influence of surface topography and surface physicochemistry on wettability of zirconia (tetragonal zirconia polycrystal). *J. Biomed. Mater. Res. B. Appl. Biomater.* **101**, 355–363. <https://doi.org/10.1002/jbm.b.32846> (2013).
- Lima, R. B. W. *et al.* Effect of silane and MDP-based primers on physico-chemical properties of zirconia and its bond strength to resin cement. *Dent. Mater.* **35**, 1557–1567. <https://doi.org/10.1016/j.dental.2019.07.008> (2019).
- Guo, W. *et al.* Effect of airborne hydrocarbons on the wettability of phase change nanoparticle decorated surfaces. *ACS Nano* **13**, 13430–13438. <https://doi.org/10.1021/acsnano.9b06909> (2019).
- Chau, T. T., Bruckard, W. J., Koh, P. T. L. & Nguyen, A. V. A review of factors that affect contact angle and implications for flotation practice. *Adv. Colloid Interface Sci.* **150**, 106–115. <https://doi.org/10.1016/j.cis.2009.07.003> (2009).
- Rupp, F. *et al.* A review on the wettability of dental implant surfaces I: Theoretical and experimental aspects. *Acta Biomater.* **10**, 2894–2906. <https://doi.org/10.1016/j.actbio.2014.02.040> (2014).
- Kuznetsov, G. V. *et al.* Influence of roughness on polar and dispersed components of surface free energy and wettability properties of copper and steel surfaces. *Surf. Coat. Technol.* **422**, 127518. <https://doi.org/10.1016/j.surfcoat.2021.127518> (2021).
- Zahran, R., Rosales Leal, J. I., Rodríguez Valverde, M. A. & Cabrerizo Vilchez, M. A. Effect of hydrofluoric acid etching time on Titanium topography, chemistry, wettability, and cell adhesion. *PLoS One*. **11**, e0165296. <https://doi.org/10.1371/journal.pone.0165296> (2016).
- Foadi, F., ten Brink, G., Mohammadzadeh, M. R. & Palasantzas, G. Roughness dependent wettability of sputtered copper thin films: The effect of the local surface slope. *J. Appl. Phys.* **125**, 244307. <https://doi.org/10.1063/1.5092672> (2019).
- Yang, Q. *et al.* Investigating the correlation between surface wettability and morphology parameters of femtosecond laser processed on YT15. *J. Laser Appl.* **33**, 012025. <https://doi.org/10.2351/7.0000237> (2020).
- Zhang, Q. *et al.* Evaluation of surface properties and shear bond strength of zirconia substructure after sandblasting and acid etching. *Mater. Res. Express.* **7**, 095403. <https://doi.org/10.1088/2053-1591/abb5c9> (2020).
- Kim, M. *et al.* Evaluation of tensile bond strength between self-adhesive resin cement and surface-pretreated zirconia. *Materials (Basel)* **15**, 3089. <https://doi.org/10.3390/ma15093089> (2022).

38. Flores-Ferreira, B. *et al.* Effect of airborne-particle abrasion and acid and alkaline treatments on shear bond strength of dental zirconia. *Dent. Mater. J.* **38**, 182–188. <https://doi.org/10.4012/dmj.2018-078> (2019).
39. Harb, O., Al-Zordk, W., Ozcan, M. & Sakrana, A. A. Influence of hydrofluoric acid and nitric acid pre-treatment and type of adhesive cement on retention of zirconia crowns. *Materials (Basel)* **14**, 960. <https://doi.org/10.3390/ma14040960> (2021).
40. Lee, J.-H. & Lee, C.-H. Effect of the surface treatment method using airborne-particle abrasion and hydrofluoric acid on the shear bond strength of resin cement to zirconia. *Dent. J. (Basel)* **5**, 23. <https://doi.org/10.3390/dj5030023> (2017).
41. Ozcan, M., Allahbeickaraghi, A. & Dündar, M. Possible hazardous effects of hydrofluoric acid and recommendations for treatment approach: A review. *Clin. Oral. Investig.* **16**, 15–23. <https://doi.org/10.1007/s00784-011-0636-6> (2012).
42. Cotic, J., Jevnikar, P., Kocjan, A. & Kosmac, T. Complexity of the relationships between the sintering-temperature-dependent grain size, airborne-particle abrasion, ageing and strength of 3Y-TZP ceramics. *Dent. Mater.* **32**, 510–518. <https://doi.org/10.1016/j.dental.2015.12.004> (2016).
43. Okada, M., Taketa, H., Torii, Y., Irie, M. & Matsumoto, T. Optimal sandblasting conditions for conventional-type yttria-stabilized tetragonal zirconia polycrystals. *Dent. Mater.* **35**, 169–175. <https://doi.org/10.1016/j.dental.2018.11.009> (2019).
44. Chintapalli, R. K., Mestra Rodriguez, A., Garcia Marro, F. & Anglada, M. Effect of sandblasting and residual stress on strength of zirconia for restorative dentistry applications. *J. Mech. Behav. Biomed. Mater.* **29**, 126–137. <https://doi.org/10.1016/j.jmbbm.2013.09.004> (2014).
45. Yu, M. K., Oh, E. J., Lim, M. J. & Lee, K. W. Change of phase transformation and bond strength of Y-TZP with various hydrofluoric acid etching. *Restor. Dent. Endod.* **46**, e54. <https://doi.org/10.5395/rde.2021.46.e54> (2021).
46. Galvao Ribeiro, B. R., Galvao Rabelo Caldas, M. R., Almeida, A. A. Jr., Fonseca, R. G. & Adabo, G. L. Effect of surface treatments on repair with composite resin of a partially monoclinic phase transformed yttrium-stabilized tetragonal zirconia. *J. Prosthet. Dent.* **119**, 286–291. <https://doi.org/10.1016/j.prosdent.2017.02.014> (2018).
47. Thammajaruk, P., Buranadham, S., Prasansuttiporn, T. & Guazzato, M. Influence of a novel lithium disilicate coating on composite-zirconia bonding and bond characterization. *Int. J. Prosthodont.* **36**, 172–180. <https://doi.org/10.11607/ijp.6744> (2023).
48. Ramesh, S., Lee Kit Yee, S. & Tan, C. Y. A review on the hydrothermal ageing behaviour of Y-TZP ceramics. *Ceram. Int.* **44**, 20620–20634. <https://doi.org/10.1016/j.ceramint.2018.08.216> (2018).
49. Seo, S.-H., Kim, J.-E., Nam, N.-E. & Moon, H.-S. Effect of air abrasion, acid etching, and aging on the shear bond strength with resin cement to 3Y-TZP zirconia. *J. Mech. Behav. Biomed. Mater.* **134**, 105348. <https://doi.org/10.1016/j.jmbbm.2022.105348> (2022).
50. Kwon, S. M., Min, B. K., Kim, Y. K. & Kwon, T. Y. Influence of sandblasting particle size and pressure on resin bonding durability to zirconia: a residual stress study. *Materials (Basel)* **13**, 5629. <https://doi.org/10.3390/ma13245629> (2020).
51. Flamant, Q. & Anglada, M. Hydrofluoric acid etching of dental zirconia. Part 2: Effect on flexural strength and ageing behavior. *J. Eur. Ceram. Soc.* **36**, 135–145. <https://doi.org/10.1016/j.jeurceramsoc.2015.09.022> (2016).
52. Chen, C. *et al.* The effects of water on degradation of the zirconia-resin bond. *J. Dent.* **64**, 23–29. <https://doi.org/10.1016/j.jdent.2017.04.004> (2017).

Author contributions

S.W., O.T. and T.P. contributed to the study conception and design. S.W., T.P. and P.N. performed the experiment. Data collection and analysis were performed by S.W., O.T., T.P. and T.S. The first draft of the manuscript was written by S.W. and O.T., and then O.T., T.P., K.H., R.F. and M.N. revised the manuscript and contributed substantially to the discussion. All authors read and approved the final manuscript.

Competing interests

The authors declare no competing interests.

Additional information

Correspondence and requests for materials should be addressed to T.P.

Reprints and permissions information is available at www.nature.com/reprints.

Publisher's note Springer Nature remains neutral with regard to jurisdictional claims in published maps and institutional affiliations.



Open Access This article is licensed under a Creative Commons Attribution 4.0 International License, which permits use, sharing, adaptation, distribution and reproduction in any medium or format, as long as you give appropriate credit to the original author(s) and the source, provide a link to the Creative Commons licence, and indicate if changes were made. The images or other third party material in this article are included in the article's Creative Commons licence, unless indicated otherwise in a credit line to the material. If material is not included in the article's Creative Commons licence and your intended use is not permitted by statutory regulation or exceeds the permitted use, you will need to obtain permission directly from the copyright holder. To view a copy of this licence, visit <http://creativecommons.org/licenses/by/4.0/>.

© The Author(s) 2023